NEOPLASIA
www.neoplasia.com
Volume 11 Number 3 March 2009 pp. 260–268 260

Recurrent *RECQL4* Imbalance and Increased Gene Expression Levels Are Associated with Structural Chromosomal Instability in Sporadic Osteosarcoma[1,2]

Georges Maire*, Maisa Yoshimoto*, Susan Chilton-MacNeill†, Paul S. Thorner‡, Maria Zielenska†,‡ and Jeremy A. Squire*

*Department of Pathology and Molecular Medicine, Richardson Labs, Queen's University, Kingston, Ontario, Canada; †Genetics and Genome Biology, The Hospital for Sick Children, Toronto, Ontario, Canada; ‡Department of Pediatric Laboratory, Medicine and Pathobiology, The Hospital for Sick Children, Toronto, Ontario, Canada

Abstract

Osteosarcoma (OS) is an aggressive bone tumor with complex abnormal karyotypes and a highly unstable genome, exhibiting both numerical- and structural-chromosomal instability (N- and S-CIN). Chromosomal rearrangements and genomic imbalances affecting 8q24 are frequent in OS. *RECQL4* gene maps to this cytoband and encodes a putative helicase involved in the fidelity of DNA replication and repair. This protective genomic function of the protein is relevant because often patients with Rothmund-Thomson syndrome have constitutional mutations of *RECQL4* and carry a very high risk of developing OS. To determine the relative level of expression of *RECQL4* in OS, 18 sporadic tumors were studied by reverse transcription–polymerase chain reaction. All tumors overexpressed *RECQL4* in comparison to control osteoblasts, and fluorescence *in situ* hybridization analysis of tumor DNA showed that expression levels were strongly copy number–dependent. Relative N- and S-CIN levels were determined by classifying copy number transitions within array comparative genomic hybridization profiles and by enumerating the frequency of break-apart fluorescence *in situ* hybridization within 8q24 using region-specific and control probes. Although there was no evidence that disruption of 8q24 in OS led to an elevated expression of *RECQL4*, there was a marked association between increased overall levels of S-CIN, determined by copy number transition frequency and higher levels of *RECQL4*.

Neoplasia (2009) 11, 260–268

Introduction

Osteosarcoma (OS) is the most common primary bone malignancy and is characterized by complex chromosomal abnormalities that vary widely from cell to cell. These tumors exhibit a high degree of aneuploidy, gene amplification, and multiple unbalanced chromosomal rearrangements. A combined approach of molecular cytogenetics techniques [comparative genomic hybridization (CGH), spectral karyotyping, or multicolor banding] together with classic G-banded cytogenetics analysis of OS tumors describe complex karyotypes with multiple numerical and structural chromosomal aberrations. Collectively, these studies [1–12] have highlighted the unique and highly unstable karyotype of OS.

Two distinct processes governing genome stability may be disrupted in cancer cells: those that affect numerical segregation and ploidy of chromosomes and those that affect the fidelity of DNA replication/repair and lead to structural chromosome aberrations (reviewed in [13]). The complexity of the OS genome likely arises as a consequence of chromosomal instability (CIN), generated by both

Address all correspondence to: Jeremy A. Squire, PhD, Translational Laboratory Research, NCIC Clinical Trials Group, Department of Pathology and Molecular Medicine, Richardson Labs, 88 Stuart St, Queen's University, Kingston, Ontario, Canada K7L 3N6. E-mail: squirej@queensu.ca

[1]This research is supported by the Canadian Cancer Society 016215. G.M. is the recipient of the Helena Lam award.
[2]This article refers to supplementary materials, which are designated by Tables W1 and W2 and are available online at www.neoplasia.com.
Received 29 October 2008; Revised 21 December 2008; Accepted 22 December 2008

DOI 10.1593/neo.81384

numerical and structural chromosome abnormalities. Numerical patterns of chromosomal aberration have been referred to as N-CIN, whereas CIN that leads to elevated levels of structural change has been termed S-CIN. The development of high-resolution array comparative genomic hybridization (aCGH) methods provides an opportunity to analyze genomic complexity at both the N-CIN and S-CIN level using whole-genome imbalance plots. In this approach, the respective distributions of copy number alteration present within the entire aCGH profile can be used to determine the relative contributions of S-CIN [as defined by copy number transitions (CNTs) [14], within each chromosome] or N-CIN (as defined by chromosomal imbalance affecting an entire chromosome) to the overall complexity of the OS genome in a given tumor. Previously [15], we have used aCGH analysis of OS to map chromosomal regions recurrently subject to genomic changes such as gene amplification. In the current article, we further interrogate aCGH profiles to measure levels of S-CIN and N-CIN in OS in the context of genomic and molecular changes of cytoband 8q24.

Some chromosomal regions are more frequently involved in genomic aberrations in OS, namely, 1p35-p36, 6p12-p21, 8q23-q24, 17p11-p12, and 19p13 [4] (reviewed in [16]). The 8q24 region is of particular interest to OS because a number of genes both directly and indirectly implicated in OS oncogenesis map to this region. The *MYC* oncogene at 8q24 is highly amplified in a subset of OS [17,18], is overexpressed more frequently in relapsed and metastatic OS [19], and is often amplified in a wide variety of carcinomas [20]. *RECQL4* maps to this same cytoband and the gene encodes a putative helicase involved in the fidelity of DNA replication, and this protective genomic function of the protein is provocative because patients with constitutional mutations of *RECQL4* have Rothmund-Thomson syndrome (RTS) and carry a very high risk of developing an OS [21]. Approximately two-thirds of patients with a clinical diagnosis of RTS will have *RECQL4* mutations. The other one third likely represents genetic heterogeneity and have mutations in another gene(s). The RTS patients with *RECQL4* mutations have a much higher risk of developing OS compared with the RTS patients without *RECQL4* mutations [22]. Moreover, the 8q24 cytoband is now of particular interest to cancer biologists because recent genome-wide association studies have identified multiple neighboring regions within a 600-kb segment of chromosome 8q24 that harbors variants associated with predisposition to prostate, colon, and bladder cancers [23–25]. The most likely candidate gene within the 8q24 region that could contribute directly to the CIN phenotype of OS is the *RECQL4* gene, which encodes a helicase member of the RecQ family [26].

In this study, we address the hypothesis that deregulation of *RECQL4* expression, caused by the 8q24 rearrangements, could underlie the high rate of CIN observed in OS. Complex genomic alterations and amplifications at 8q24 were of particular interest because the affected regions are relatively small; they have been found to be aberrant in multiple OS samples and they are located in a region of the human genome strongly implicated in tumorigenesis and DNA repair. If genomic alterations occur near the *RECQL4* region, it is conceivable that such changes lead to deregulation of the locus, and this may compromise its repair and DNA maintenance functions, with consequences for the entire genome's integrity [26–30]. In the present study, we used 18 OS tumor samples to investigate whether *RECQL4* gene expression levels were linked to the extent and type of CIN (N-CIN and S-CIN) throughout the OS genome and specifically at 8q24.

Materials and Methods

Patient Tumors

The collection of frozen tissue specimens (n = 18), archival formalin-fixed, paraffin-embedded OS sections (n = 12), and clinicopathologic data was obtained and handled in accordance with the Hospital for Sick Children Research Ethics guideline (Toronto, Canada). The OS specimens and corresponding paraffin-embedded specimens consisted of resected or biopsy tumor tissue obtained at diagnosis. Hematoxylin and eosin–stained sample sections were subjected to standard histopathologic evaluation to determine the tumor content and the pathologic grade according to the World Health Organization [31]. All samples presented a tumor content higher than 90%. The clinical and histologic features of presented OS cohort are detailed in Table 1.

Cell Culture

The RTS primary fibroblasts were obtained from the Corriell Institute for Medical Research (AG18371; Camden, NJ) [32]. These fibroblasts do not express *RECQL4* because of an 11-bp intronic deletion, which disrupts the splicing and compromises its expression [32,33]. They were cultured in alpha–minimum essential medium (Invitrogen, Burlington, Ontario, Canada) supplemented with 10% heat-inactivated fetal calf serum (Invitrogen). Osteoblasts were obtained from PromoCell (Heidelberg, Germany) and cultured in osteoblast culture medium (PromoCell).

RNA Extraction and Semiquantitative Reverse Transcription–Polymerase Chain Reaction

The mRNA level of *RECQL4* was examined by semiquantitative reverse transcription–polymerase chain reaction (RT-PCR), using the housekeeping gene *PBGD* as a calibration control. Total RNA from snap-frozen OS tumors (18 samples) and from cultured cells (RTS fibroblasts and osteoblasts) were isolated using the TRIzol Reagent (Invitrogen). The RNA quality was assessed by BioAnalyzer RNA 600 Nano Kit (Agilent Technologies, Palo Alto, CA). Total RNA from kidney and testis (Ambion, Foster City, CA) were used as positive control detection for low and high *RECQL4* expressions, respectively [34]. Total RNA from RTS fibroblasts were used as negative control [33,35]. Coamplification of *RECQL4* and *PBGD* genes

Table 1. Clinical Data of the 18 OSs.

No.	Sex	Age (years)	Localization	Sample	Subtype	Grade
OS1	F	9	Tibia	Biopsy	Osteoblastic	High
OS2	M	14	Femur	Lesion	Osteoblastic	High
OS3	M	13	Femur	Biopsy	Osteoblastic	Intermediate
OS4	M	7	Humerus	Biopsy	Poorly differentiated	High
OS5	F	12	Femur	Biopsy	Poorly differentiated	High
OS6	M	14	Femur	Biopsy	Osteoblastic	High
OS7	M	7	Femur	Biopsy	Osteoblastic	High
OS8	M	13	Femur	Resection	Osteoblastic	High
OS9	F	13	Humerus	Biopsy	Osteoblastic	High
OS10	M	8	Tibia	Resection	Osteoblastic	High
OS11	M	13	Femur	Biopsy	Osteoblastic	High
OS12	M	17	Lung	Resection	Osteoblastic	High
OS13	M	9	Leg	Biopsy	Poorly differentiated	High
OS14	F	12	Femur	Biopsy	Osteoblastic	Intermediate
OS15	F	14	Femur	Biopsy	Osteoblastic	High
OS16	F	17	Tibia	Resection	Osteoblastic	High
OS17	M	15	Tibia	Resection	Osteoblastic	High
OS18	M	15	Femur	Biopsy	Poorly differentiated	High

F indicates female; *M*, male.

was performed on 150 ng of total RNA by applying the one-step RT-PCR method (Superscript One-Step RT-PCR III; Invitrogen) according to the manufacturer's instructions. *RECQL4* forward (5′-CTCATCTAAGGCATCCACCC-3′) and reverse (5′-CTGTGACATCGCTGTAACCA-3′) primers were designed to amplify a 188-bp fragment (Accession Number NM_004260). *PBGD* primers were designed to amplify a 127-bp fragment [36]. Primers for *RECQL4* and *PBGD* were combined as follows: 0.2 μM of each forward and reverse *RECQL4* primers and 0.15 μM of each forward and reverse *PBGD* primers. The reverse transcription and amplification conditions were performed using the MJ Research PTC200 thermocycler and consisted of an initial reverse transcription reaction at 57°C for 30 minutes, followed by denaturation (2 minutes at 94°C) and 30 cycles of amplification (94°C for 30 seconds; 57°C for 30 seconds; 68°C for 30 seconds). The final elongation reaction was performed at 68°C for 10 minutes. Genomic DNA contamination in every sample was excluded by omitting the reverse transcriptase in the RT-PCR.

The measurement and quantification of the 188-bp (*RECQL4*) and 127-bp (*PBGD*) coamplified fragments were performed using the DNA 1000 LabChip Kit (Agilent 2100 Bioanalyzer; Agilent Technologies) and the 2100 Expert Software (Agilent Technologies), respectively. *PBGD* was used for calibration, and the mRNA fold change of *RECQL4* in OS cohort was compared with the normal osteoblasts. The SD from triplicate RT-PCR experiments was calculated for each sample.

Genome-wide Analysis of Chromosomal Instability

Ten OS samples for which sufficient total DNA could be extracted were hybridized against Human Genome CGH 44k microarrays (Agilent Technologies), spanning the entire human genome at a median resolution of 75 kb as described previously [15]. These aCGH data files have also been used to map the distribution of recurrently deleted and amplified regions in OS [15] and they are deposited in National Center for Biotechnology Information's Gene Expression Omnibus (GEO) Web site (http://www.ncbi.nlm.nih.gov/geo/) and are accessible through the GEO Series accession number GSE9654. For each tumor, the normalized data were run through the Circular Binary Segmentation (CBS) algorithm [37], with a threshold of 0.5 (CGH Analytics, 3.5.14; Agilent Technologies). The CBS algorithm provides a list of aberrations (imbalanced genomic region with a unique abnormal CGH ratio), each determined by two CNTs, as defined by Ferreira et al. [14]. The distribution along the chromosome of these CNTs for each aberration was used to determine the respective contribution of N-CIN and S-CIN (Table W1). Briefly, an aberration with the starting and ending CNTs positioned within an arm of a chromosome was considered to be caused by copy number change arising from an unbalanced structural alteration and was scored as S-CIN. An aberration, which CNTs were positioned in telomeric or centromeric regions, was considered to result from copy number change affecting an entire chromosome or chromosome arm and was scored as N-CIN. All the aberrations were classified as N- or S-CIN–related and scored for each of the 10 OS tumors studied by aCGH. The aberrations on X and Y chromosomes were excluded from the analysis to eliminate the sex mismatching bias.

Fluorescence In Situ *Hybridization*

Dual-color fluorescence *in situ* hybridization (FISH) method was applied to the 5-μm thick archival formalin-fixed, paraffin-embedded tissue sections. Bacterial artificial chromosome (BAC) genomic clone RP11-349C2 was identified in the Resources for Molecular Cytogenetics database (www.biologia.uniba.it) by its location at the *RECQL4* locus (chr8:145,707,623-145,713,976, UCSC genome browser, www.genome.ucsc.edu, version March 2006). The BAC clone was obtained from the Centre for Applied Genomics (Toronto, Ontario, Canada). The presence of the *RECQL4* sequence and the correct chromosome location of the BAC clone were verified by PCR and by hybridization to metaphase spreads from normal peripheral lymphocytes, respectively. The BAC probe was labeled either with ULYSIS-Alexa-594 or with ULYSIS-Oregon-green-488 (Molecular Probes, Invitrogen) and was combined with the alpha satellite centromeric probe of chromosome 8, cen(8) (CEP 8 SpectrumGreen; Abbott Molecular, Des Plaines, IL) or with a commercial *MYC*-containing probe (LSI C-MYC-SpectrumOrange; Abbott Molecular), respectively. Dual-color FISH was performed according to standard procedures [38]. Either *RECQL4* and cen(8) or *RECQL4* and *MYC* were evaluated by spot visualization and enumeration for each probe in a range from 50 to 100 nonoverlapped, intact interphase nuclei per tumor tissue using a Zeiss Imager.Z1 microscope equipped with a digital camera AxioCam MRm and AxioVision 4.3 capturing software (Carl Zeiss Canada, Ltd., Toronto, Canada). If fluorescent signals could not be seen in at least 80% of cells, the result was considered to be noninterpretable (6/12). The most represented pattern of signal was recorded for the probe combinations mentioned above. The establishment of a cutoff value of >10% of tumor nuclei for the different probes used and for all signal patterns was defined considering the truncation artifacts, aneusomy, nuclear size, and chromatin condensation [39]. The relative gene copy number of *RECQL4* was calculated by adding the number of *RECQL4* signals to the *RECQL4*/cen(8) ratio. This calculation allowed to enhance the distinction between a ratio of 1 with two copies of each probe (2:2), and a ratio of 1 with three to five copies of each probe (3:3, 4:4, and 5:5). The pattern of signals (contiguous *vs* scattered) for the dual-color FISH experiment using *RECQL4* and *MYC* probes was evaluated nucleus by nucleus to document the S-CIN of the 8q24 region. The observation of scattered signals was interpreted as the manifestation of S-CIN.

Chromosome copy number analysis was performed using centromeric enumeration probes for cen(3) (CEP 3 SpectrumRed), cen(7) (CEP 7 SpectrumGreen), and cen(17) (CEP 17 SpectrumAqua; Abbott Molecular). Sequential three-color FISH method was applied to the paraffin-embedded tissue sections according to the manufacturer's instructions. Chromosome enumeration was determined by scoring the number of signals for cen(3), cen(7), and cen(17) in 200 nonoverlapped intact interphase nuclei (10 of the 12 samples reached these criteria). The estimation of the overall ploidy of each sample is described case by case in the supplementary material (Table W2). Briefly, adapted from Rossi et al. [40], the OS cohort was classified by ploidy FISH as follows: 1) diploid, >50% of cells showing two signals for all probes; 2) near-triploid, >20% of cells showing three signals for at least two probes; 3) near-tetraploid, >20% of cells showing four signal for at least two probes; 4) polyploidy, >50% of cells showing more than five signals for at least one probe [40].

Results

RECQL4 *Expression Levels in OS Determined by RT-PCR Analysis*

To establish the expression level of *RECQL4* in OS samples, we performed semiquantitative RT-PCR using total RNA extracted from

patient tumors. We demonstrated that *RECQL4* was overexpressed in all the tested tumors compared with normal osteoblasts. The mean expression levels observed for all 18 OS tumors was ~13-fold higher than osteoblasts (range, ×3 to ×30; Figure 1). In keeping with the published literature, *RECQL4* could not be detected in RNA-derived RTS fibroblasts [33,35]. OS1 exhibited the lowest level of *RECQL4* expression, which was comparable to the low expression level observed in normal kidney tissue. In contrast, OS18 was characterized by an expression twice higher than that of the normal testis sample, which has been shown to be one of the most *RECQL4*-rich tissues [34]. We conclude that the expression level of *RECQL4* is deregulated in OS.

Association of RECQL4 *Expression and Genome-wide Chromosomal Instability Levels*

To determine whether there was a relationship between expression levels of *RECQL4* and overall levels of CIN, we analyzed aCGH profiles to distinguish between N-CIN and S-CIN using 10 of the 18 tumors. Analysis of CNT distributions within each chromosome and the pattern of overall chromosomal imbalance present in each aCGH profile provided an objective overview of the variation in N-CIN and S-CIN levels that characterized each of the 10 OS analyzed (Table W1 and Figure 2). The mean number of N-CIN changes was 10.4 (SD, 5) for the study group, with no apparent relationship between the levels of *RECQL4* expression and N-CIN (Figure 2*A*). In contrast, there was a clear trend showing an increase in S-CIN with higher expression levels of *RECQL4*. For example, OS18 had the highest expression level and exhibited >300 S-CIN aberrations and OS1 showed the lowest-expressing tumor for *RECQL4* and had only 11 S-CIN aberrations. The mean number of S-CIN for the study group was 74.1 (SD, 95; Figure 2*B*). Collectively, these data indicate that elevated *RECQL4* expression is associated with a greater incidence of CNTs and concomitant elevation in S-CIN frequency. We were not able to demonstrate any relationship between N-CIN levels and varying levels of gene expression of *RECQL4*.

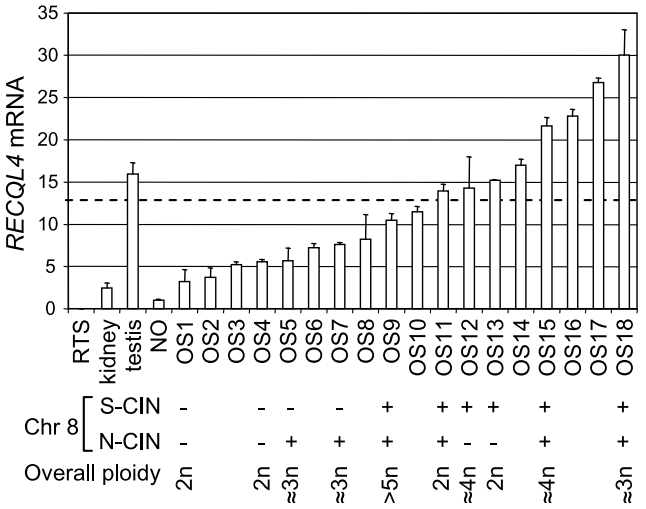

Figure 1. *RECQL4* is overexpressed in OS and is associated with S-CIN. The histogram is showing the fold change of *RECQL4* mRNA compared with normal osteoblasts (NO) measured by semiquantitative RT-PCR. Rothmund-Thomson fibroblasts (RTS) and normal tissues (kidney and testis) were used as negative and positive controls, respectively. Each value is the result of three independent experiments. The SD is shown above each bar. The dashed line represents the mean value calculated from OS sample data. The lower panel part describes the chromosomal 8 instability (CIN) in the context of overall ploidy for 10 samples for which material was available for FISH studies. The absence of N-CIN or S-CIN is shown as (−). Identification of S-CIN or N-CIN is shown as (+). The overall ploidy status was established according to the FISH data using cen(3), cen(7), and cen(17). OS tumors that are showing an *RECQL4* expression value close or more than the mean are showing S-CIN, whereas the ones less than the mean do not. The N-CIN and S-CIN are independent, and a high level of *RECQL4* expression is associated with the appearance of S-CIN on the 8q24 region.

Influence of RECQL4 *Gene Copy Number on Its Expression in OS*

The variation of the *RECQL4* expression in OS could be the result of genomic copy number changes of the locus at 8q24. Dual-color interphase FISH analysis, using the *RECQL4* and the cen(8) probes, was therefore performed on formalin-fixed, paraffin-embedded tissue derived from 12 OS tumors. As illustrated in Figure 3, *A*–*D*, and summarized in Table 2, we show that the increase of *RECQL4* expression followed the genomic status of the *RECQL4* gene. To determine copy number changes, cohybridization of *RECQL4* and cen(8) probes and systematic analysis of the dual-color patterns allowed us to quantify numerical chromosome 8 abnormalities. OS samples with the lowest expression of *RECQL4* (such as OS1 and OS4) have two normal chromosome 8s each bearing two copies of *RECQL4* and cen(8) (Figure 3*A*). In OS2, four cen(8)s were present with only two copies of the *RECQL4* gene, suggesting that a tetrasomy of chromosome 8 also involved *RECQL4* loss (Figure 3*B*). OS5, OS7, and OS9 had a higher expression of *RECQL4* (below the mean value) and three to five copies for each *RECQL4* and cen(8) probes (Figure 3, *C* and *D*). This pattern could be interpreted as an acquisition of extra copies of an intact chromosome 8. Lastly, OS samples with the highest *RECQL4* expression, (above the mean) all exhibited a copy number gain of *RECQL4*, which was observed as nine *RECQL4* signals with four cen(8) for OS15 (Figure 3*E*) or six *RECQL4* signals for two cen(8) as in OS13 (Figure 3*F*). Collectively, these findings indicate that of *RECQL4* gene expression is largely copy number–dependent (Table 2).

Influence of Structural Alterations of Cytoband 8q24 on RECQL4 *Expression in OS*

We used dual-color interphase FISH to study S-CIN levels within 8q24.21 (*MYC* probe) and 8q24.4 (*RECQL4* probe) cytobands. Because both probes are closely linked within 8q24, paired two-color signals within nuclei can be used to determine whether disruption of the cytoband has taken place. In four OS tumors (OS1, OS4, OS5, and OS7), there was no evidence of disruption between *MYC* and the *RECQL4* probes within nuclei (Table 3 and Figure 3, *G* and *H*). For six OS tumors, disruption of 8q24 was apparent. In OS13 (Figure 3*I*), six copies of 8q24 were apparent, but the red and green signals were no longer paired, indicative of structural rearrangement between the *MYC* and *RECQL4* loci. In OS15 (Figure 3*J*), we observed the most complex signal pattern in the series; no pairing of green and red signals was apparent, and there was also evidence of numerical change. Thus, a range of structural aberrations affecting 8q24, varying from simple to complex, was apparent within this

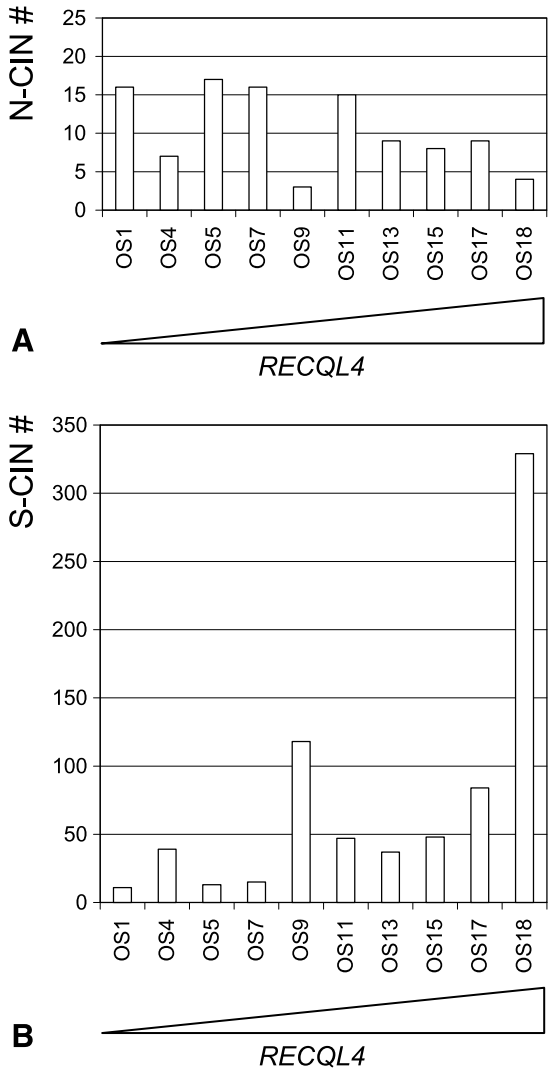

Figure 2. Association between *RECQL4* expression levels and varying N-CIN and S-CIN frequencies. (A) Differing frequencies of N-CIN (*y*-axis) as determined by analyzing imbalance profiles of whole chromosomes or entire arms for the 10 OS tumors (*x*-axis) after aCGH analysis. (B) Differing frequencies of S-CIN (*y*-axis) as determined by analyzing CNT distributions across each genomic profile derived from the ten OS tumors (*x*-axis) after aCGH analysis. The OS samples are ordered from left to right according to their *RECQL4* expression level (lowest to highest) and are represented as a triangle in which the adjacent side represents the highest *RECQL4* expression level.

series of OS tumors. The varying levels of both N-CIN and S-CIN in the 10 OS as determined by FISH analyses of 8q24 with probes are detailed in Table 3. OS1 and OS4 did not exhibit numerical or 8q24 structural aberrations. OS5 and OS7 were both characterized by N-CIN only, whereas OS12 and OS13 had S-CIN only. The largest

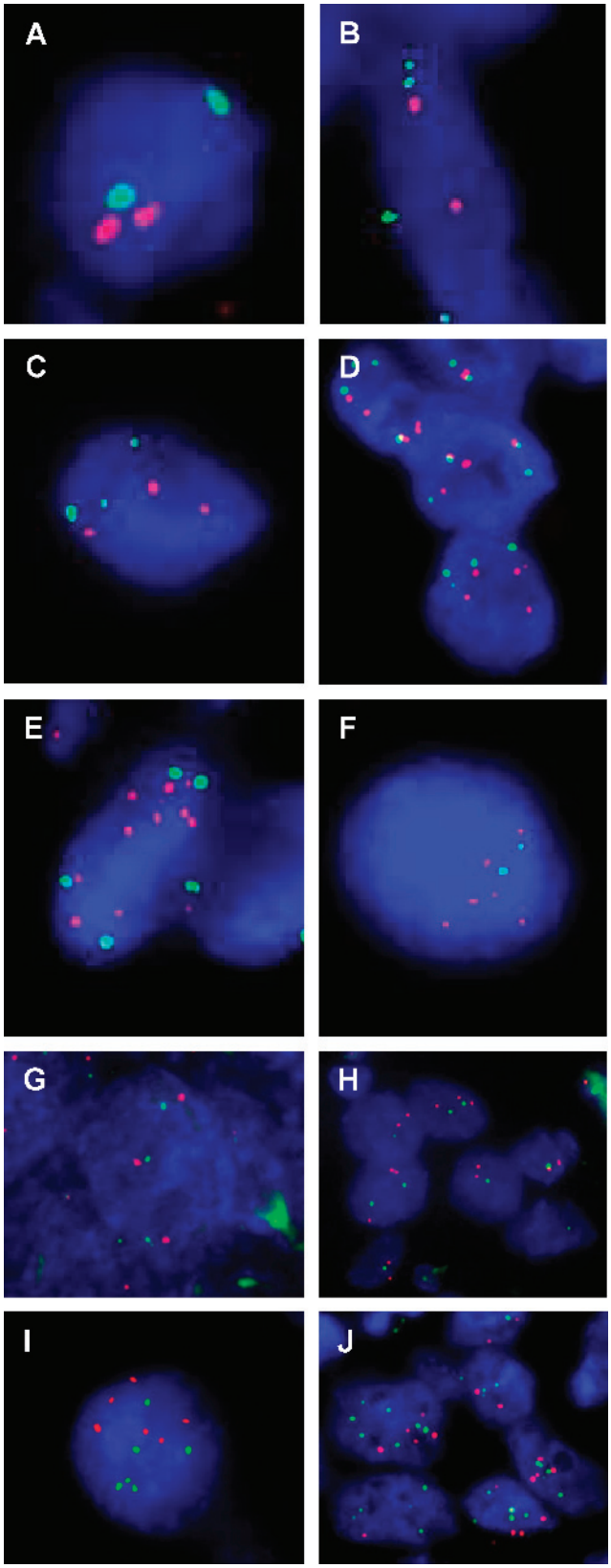

Figure 3. (A–F) *RECQL4*/cen(8) dual-color interphase FISH experiment on OS tumors samples' fixed sections. *RECQL4* probe is shown in red, whereas the cen(8) is in green. OS samples exhibited a normal pattern [OS1 (A)], a loss [OS2 (B)], an abnormal pattern associated with a 1:1 ratio [OS7 (C) and OS9 (D)], or a gain of *RECQL4* [OS15 (E) and OS13 (F)]. (G–J) Structural CIN of the 8q24 cytoband. Dual-color interphase FISH was done on fixed tissue sections using the *MYC* probe (red) located on 8q24.21 and the RP11-349C2 probe (green) located on 8q24.3. The signal pattern of contiguous red and green signals on OS7 (G) and OS1 (H) identifies these samples as no S-CIN for the 8q24 cytoband. In contrast, for OS13 (I) and OS15 (J), the red and green signals are scattered all around the nuclei, characterizing these two samples as S-CIN for the 8q24 region.

Table 2. *RECQL4* Relative Gene Copy Number and Expression Analysis.

No.	*RECQL4* Copy Number (Genomic Status)	cen(8) Copy Number	*RECQL4* Relative Copy Number*	*RECQL4* Expression (Fold Change)†
OS1	2 (N)	2	3	3
OS2	2 (L)	4	2.5	4
OS4	2 (N)	2	3	6
OS5	4 (AN)	4	5	6
OS7	3 (AN)	3	4	8
OS9	5 (AN)	5	6	10
OS11	6 (G)	4	7.5	14
OS12	3 (G)	2	4.5	14
OS13	6 (G)	2	9	15
OS15	8 (G)	4	10	22
OS16	9 (G)	2	13.5	23
OS18	5 (G)	3	6.6	30

AN indicates aneusomy; *G*, gain; *L*, loss; *N*, normal.
**RECQL4* relative number is calculated as described in the Materials and Methods section.
†Expression of *RECQL4* is normalized against the *PBGD* housekeeping gene expression, and shown as a fold change compared with the expression level measured in normal osteoblasts.

group of tumors, OS9, OS11, OS15, and OS18 had more complex FISH patterns, with both N- and S-CIN occurring together at 8q24. We then compared *RECQL4* expression findings in tumors with N- or S-CIN at 8q24 to determine whether expression levels were associated with numerical or structural alterations of this region of chromosome 8. OS tumors with *RECQL4* expression values that were close or higher than the mean value (13.5) across the 18 OS samples had S-CIN for the 8q24 region. This relationship held regardless of the N-CIN level or ploidy for chromosome 8 (Figure 1). Moreover, OS with the highest S-CIN levels determined by aCGH (shown above) also had the highest S-CIN level with the 8q24 cytoband region. These findings do not indicate that disruption of 8q24 leads to elevated expression of *RECQL4 per se*; rather, elevated *RECQL4* is strongly associated with a greater overall frequency of S-CIN.

Discussion

Previous studies of the *RECQL4* gene have shown a strong association between constitutional mutations of the locus and predisposition to OS with 32% of RTS patient developing OS [22]. Moreover, fibroblasts and lymphocytes from RTS exhibit both N- and S-CIN [41–45]. Sequence analyses of *RECQL4* in a large series of sporadic OS tumors failed to detect mutations in a significant proportion (only 3 samples of 71 had mutation/deletion) [46], but no study to date has determined the *RECQL4* genomic status or analyzed expression levels in the context of CIN in OS.

The biologic function of the RECQL4 protein is poorly understood. The extensive studies of RTS, BLM and WRN, and other members of the RecQ helicase family, have not provided conclusive information concerning the specific and diverse functions of the RECQL4 protein. It is clear that for all three syndromes, germ line mutation of a specific RecQ helicase gene is associated with premature aging, CIN, and predisposition to diverse types of cancer [47]. However, there are important clinical and biologic differences between these genes. For example, conserved areas of the RECQL4 and BLM helicase motif do not have functional equivalence *in vitro* [27]. Each syndrome has distinct clinical features, and the associated cancer risk involves a different spectrum of tumors [48–50]. Moreover, the prominent class of CIN observed in the lymphocytes or fibroblasts of each syndrome varies, with RTS being characterized by chromatid breaks and isochromosomes, BLM by triradial and quadriradial figures, and WRN by multiple clones with distinctive balance translocations [50–52]. Interestingly, recent characterization of the overexpression of the RecQ helicases has shown it to be linked with the deregulation of the Rb pathway and the RAS activation. These data provide additional support to our supposition that there is an association between oncogenesis and RecQ helicases' overexpression [53]. In the proposed model, RecQ helicases' overexpression

Table 3. Relative Levels of Numerical and Structural Chromosomal Instability in 10 OSs.

No.	Numerical Aberration		Structural Aberration of Chromosome 8			Type of CIN for Chromosome 8
	Overall Ploidy*	cen(8)	*RECQL4* Copy Number	*MYC* Copy Number	Pattern of *RECQL4* and *MYC* FISH Signals	
OS1	Diploid	2	2	3	Not rearranged	—
OS4	Diploid	2	2	2	Not rearranged	—
OS5	Near-triploid	4	4	4	Not rearranged	N-CIN
OS7	Near-triploid	3	3	3	Not rearranged	N-CIN
OS9	Polyploid (>5n)	5	4	4	Scattered	S- and N-CIN
OS11	Diploid	4	6	4	Scattered	S- and N-CIN
OS12	Near-tetraploid	2	3	2	Scattered	S-CIN
OS13	Diploid	2	6	6	Scattered	S-CIN
OS15	Near-tetraploid	4	8	5	Scattered	S- and N-CIN
OS18	Near-triploid	3	5	3	Scattered	S- and N-CIN

CIN indicates chromosomal instability; *N-CIN*, numerical chromosomal instability; *S-CIN*, structural chromosomal instability.
**The overall ploidy has been estimated by the enumeration of cen(3), cen(7), and cen(17) (Table W2) as described in the Materials and Methods section.*

would promote and facilitate the DNA synthesis and telomere maintenance, processes that are mandatory for any transformed cells. However, similar to the different effects of the WRN, BLM, or RECQL4 mutations, the regulation of the RecQ helicase seems to be specific for each of the member [53]. In the last few years, several groups identified a more specific function for the RECQL4 helicase, specially its involvement in the early steps of replication fork machinery [27–30]. In an animal model, Sangrithi et al. [28] showed that the *Xenopus laevi* RECQL4 homolog is associated with chromatin during replication initiation and makes the origin of replication accessible to the replication factors. This function acts on the initiation and the unraveling of single-stranded DNA at the origin of replication. An altered expression of RECQL4 could disturb the processes governing the duration and extent of single-strand DNA exposure. Therefore, these single-stranded DNA regions would be the targets of DNA fragility and breaks. This abnormal single configuration of DNA is likely to promote interchromosome exchanges in a pseudo homolog recombination way. Because RECQL4 is activated by single-strand DNA and it promotes annealing of single-strand DNA to its complementary sequence, an excess of RECQL4 could force unmatched DNA annealing sequence, whereas a lack of RECQL4 could impair proper reannealing of separated strands of DNA [27]. Thus, the deregulation of RECQL4 could have profound consequences on overall genomic integrity and CIN in terms of structural complexity and heterogeneity.

By mapping the distribution of regions of imbalance and, in particular, determining the location of CNTs (Table W1) within each chromosome, it is possible to evaluate the relative contributions of N-CIN and S-CIN to destabilizing the OS genome. In this study, we have found that elevated *RECQL4* expression is associated with a greater overall frequency of structural chromosomal change, but there was no obvious relationship between expression and N-CIN levels (Figure 2). Moreover, S-CIN changes were also apparent when FISH was used to determine the frequency of structural alteration at cytoband 8q24. It is possible that the elevated levels of *RECQL4* would keep the DNA in a prolonged single stranded vulnerable stage, and promote the S-CIN. A result of this deregulation would be the perpetual initiation of S-CIN, leading to a polyclonal population of cells within one tumor. Indeed, OS tumor can exhibit highly polyclonal population where the most represented clone could account for only 30% of the cell [2–4].

Overexpression of *RECQL4* has also been reported in other sarcomas (leiomyosarcoma, liposarcoma, and synovial sarcoma) and in some carcinomas (breast, colon, cervix, and laryngeal squamous cells), and its elevated expression has been correlated with metastasis or a later stage of disease [54–58]. Of these tumors, none have been studied systematically to determine whether S-CIN levels are elevated. However, in liposarcoma, the presence of a supernumerary giant chromosomes that varies structurally from cell to cell suggests ongoing instability [59]. These observations would give *RECQL4* a strong impact in oncogenesis in general. In the present study, the *MYC* amplicon (8q24.21) seems to be independent of from the *RECQL4* locus (8q24.3). The study by Mai and Mushinski [60] suggests that amplification and deregulation of MYC lead to instability characterized by gene amplification rather than by elevated frequencies of structural chromosomal rearrangement. This would be consistent with our finding: we observed a disruption of the 8q24 cytoband rather than an over–replication/amplification pattern (Figure 3, *I* and *J*), as one would expect as a result of an MYC-driven S-CIN in a given tumor. Furthermore, MYC is a multifunctional protein that acts on cell cycle, apoptosis, and cellular transformation through its transcription factor activity [20]. Conversely, RECQL4 seems to be more involved in specific DNA metabolism. We therefore suggest that the imbalances of the *MYC* oncogene and *RECQL4* are two independent processes of oncogenesis.

In this study, we have investigated the relationship between S-CIN/N-CIN in OS and the RNA expression levels of *RECQL4*. We find that whereas ploidy changes and elevated N-CIN is common in OS, the more structurally abnormal tumors have higher levels of *RECQL4*. OS with the highest S-CIN levels determined by aCGH also had the highest S-CIN level with the 8q24 cytoband region. We found no evidence that disruption of 8q24 led to an elevated expression of *RECQL4*; rather, elevated *RECQL4* is strongly associated with a greater overall frequency of S-CIN that characterizes the OS genome.

Acknowledgments

The authors thank Olga Ludkovski (Ontario Cancer Institute, Toronto, Canada) for her technical assistance for the enumeration FISH experiments.

References

[1] Bridge JA, Nelson M, McComb E, McGuire MH, Rosenthal H, Vergara G, Maale GE, Spanier S, and Neff JR (1997). Cytogenetic findings in 73 osteosarcoma specimens and a review of the literature. *Cancer Genet Cytogenet* **95**, 74–87.

[2] Zielenska M, Bayani J, Pandita A, Toledo S, Marrano P, Andrade J, Petrilli A, Thorner P, Sorensen P, and Squire JA (2001). Comparative genomic hybridization analysis identifies gains of 1p35 approximately p36 and chromosome 19 in osteosarcoma. *Cancer Genet Cytogenet* **130**, 14–21.

[3] Squire JA, Pei J, Marrano P, Beheshti B, Bayani J, Lim G, Moldovan L, and Zielenska M (2003). High-resolution mapping of amplifications and deletions in pediatric osteosarcoma by use of CGH analysis of cDNA microarrays. *Genes Chromosomes Cancer* **38**, 215–225.

[4] Bayani J, Zielenska M, Pandita A, Al-Romaih K, Karaskova J, Harrison K, Bridge JA, Sorensen P, Thorner P, and Squire JA (2003). Spectral karyotyping identifies recurrent complex rearrangements of chromosomes 8, 17, and 20 in osteosarcomas. *Genes Chromosomes Cancer* **36**, 7–16.

[5] Ozaki T, Neumann T, Wai D, Schafer KL, van Valen F, Lindner N, Scheel C, Bocker W, Winkelmann W, Dockhorn-Dworniczak B, et al. (2003). Chromosomal alterations in osteosarcoma cell lines revealed by comparative genomic hybridization and multicolor karyotyping. *Cancer Genet Cytogenet* **140**, 145–152.

[6] Lim G, Karaskova J, Vukovic B, Bayani J, Beheshti B, Bernardini M, Squire JA, and Zielenska M (2004). Combined spectral karyotyping, multicolor banding, and microarray comparative genomic hybridization analysis provides a detailed characterization of complex structural chromosomal rearrangements associated with gene amplification in the osteosarcoma cell line MG-63. *Cancer Genet Cytogenet* **153**, 158–164.

[7] Lim G, Karaskova J, Beheshti B, Vukovic B, Bayani J, Selvarajah S, Watson SK, Lam WL, Zielenska M, and Squire JA (2005). An integrated mBAND and submegabase resolution tiling set (SMRT) CGH array analysis of focal amplification, microdeletions, and ladder structures consistent with breakage-fusion-bridge cycle events in osteosarcoma. *Genes Chromosomes Cancer* **42**, 392–403.

[8] Atiye J, Wolf M, Kaur S, Monni O, Bohling T, Kivioja A, Tas E, Serra M, Tarkkanen M, and Knuutila S (2005). Gene amplifications in osteosarcoma-CGH microarray analysis. *Genes Chromosomes Cancer* **42**, 158–163.

[9] Man TK, Lu XY, Jaeweon K, Perlaky L, Harris CP, Shah S, Ladanyi M, Gorlick R, Lau CC, and Rao PH (2004). Genome-wide array comparative genomic hybridization analysis reveals distinct amplifications in osteosarcoma. *BMC Cancer* **4**, 45.

[10] van Dartel M, Cornelissen PW, Redeker S, Tarkkanen M, Knuutila S, Hogendoorn PC, Westerveld A, Gomes I, Bras J, and Hulsebos TJ (2002). Amplification of 17p11.2 approximately p12, including PMP22, TOP3A, and MAPK7, in high-grade osteosarcoma. *Cancer Genet Cytogenet* **139**, 91–96.

[11] Selvarajah S, Yoshimoto M, Maire G, Paderova J, Bayani J, Squire JA, and Zielenska M (2007). Identification of cryptic microaberrations in osteosarcoma

by high-definition oligonucleotide array comparative genomic hybridization. *Cancer Genet Cytogenet* **179**, 52–61.

[12] Sandberg AA and Bridge JA (2003). Updates on the cytogenetics and molecular genetics of bone and soft tissue tumors: osteosarcoma and related tumors. *Cancer Genet Cytogenet* **145**, 1–30.

[13] Bayani J, Selvarajah S, Maire G, Vukovic B, Al-Romaih K, Zielenska M, and Squire JA (2007). Genomic mechanisms and measurement of structural and numerical instability in cancer cells. *Semin Cancer Biol* **17**, 5–18.

[14] Ferreira BI, Alonso J, Carrillo J, Acquadro F, Largo C, Suela J, Teixeira MR, Cerveira N, Molares A, Gomez-Lopez G, et al. (2008). Array CGH and gene-expression profiling reveals distinct genomic instability patterns associated with DNA repair and cell-cycle checkpoint pathways in Ewing's sarcoma. *Oncogene* **27**, 2084–2090.

[15] Selvarajah S, Yoshimoto M, Ludkovski O, Park PC, Bayani J, Thorner P, Maire G, Squire JA, and Zielenska M (2008). Genomic signatures of chromosomal instability and osteosarcoma progression detected by high resolution array CGH and interphase FISH. *Cytogenet Genome Res* **122**, 5–15.

[16] Baudis M (2006). Online database and bioinformatics toolbox to support data mining in cancer cytogenetics. *Biotechniques* **40**, 269–270; 272.

[17] Ladanyi M, Park CK, Lewis R, Jhanwar SC, Healey JH, and Huvos AG (1993). Sporadic amplification of the *MYC* gene in human osteosarcomas. *Diagn Mol Pathol* **2**, 163–167.

[18] Stock C, Kager L, Fink FM, Gadner H, and Ambros PF (2000). Chromosomal regions involved in the pathogenesis of osteosarcomas. *Genes Chromosomes Cancer* **28**, 329–336.

[19] Gamberi G, Benassi MS, Bohling T, Ragazzini P, Molendini L, Sollazzo MR, Pompetti F, Merli M, Magagnoli G, Balladelli A, et al. (1998). C-*myc* and c-*fos* in human osteosarcoma: prognostic value of mRNA and protein expression. *Oncology* **55**, 556–563.

[20] Oster SK, Ho CS, Soucie EL, and Penn LZ (2002). The *myc* oncogene: MarvelouslY Complex. *Adv Cancer Res* **84**, 81–154.

[21] Wang LL, Levy ML, Lewis RA, Chintagumpala MM, Lev D, Rogers M, and Plon SE (2001). Clinical manifestations in a cohort of 41 Rothmund-Thomson syndrome patients. *Am J Med Genet* **102**, 11–17.

[22] Wang LL, Gannavarapu A, Kozinetz CA, Levy ML, Lewis RA, Chintagumpala MM, Ruiz-Maldanado R, Contreras-Ruiz J, Cunniff C, Erickson RP, et al. (2003). Association between osteosarcoma and deleterious mutations in the *RECQL4* gene in Rothmund-Thomson syndrome. *J Natl Cancer Inst* **95**, 669–674.

[23] Poynter JN, Figueiredo JC, Conti DV, Kennedy K, Gallinger S, Siegmund KD, Casey G, Thibodeau SN, Jenkins MA, Hopper JL, et al. (2007). Variants on 9p24 and 8q24 are associated with risk of colorectal cancer: results from the Colon Cancer Family Registry. *Cancer Res* **67**, 11128–11132.

[24] Haiman CA, Patterson N, Freedman ML, Myers SR, Pike MC, Waliszewska A, Neubauer J, Tandon A, Schirmer C, McDonald GJ, et al. (2007). Multiple regions within 8q24 independently affect risk for prostate cancer. *Nat Genet* **39**, 638–644.

[25] Kiemeney LA, Thorlacius S, Sulem P, Geller F, Aben KK, Stacey SN, Gudmundsson J, Jakobsdottir M, Bergthorsson JT, Sigurdsson A, et al. (2008). Sequence variant on 8q24 confers susceptibility to urinary bladder cancer. *Nat Genet* **40**, 1307–1312.

[26] Sharma S, Doherty KM, and Brosh RM Jr (2006). Mechanisms of RecQ helicases in pathways of DNA metabolism and maintenance of genomic stability. *Biochem J* **398**, 319–337.

[27] Macris MA, Krejci L, Bussen W, Shimamoto A, and Sung P (2006). Biochemical characterization of the RECQ4 protein, mutated in Rothmund-Thomson syndrome. *DNA Repair (Amst)* **5**, 172–180.

[28] Sangrithi MN, Bernal JA, Madine M, Philpott A, Lee J, Dunphy WG, and Venkitaraman AR (2005). Initiation of DNA replication requires the RECQL4 protein mutated in Rothmund-Thomson syndrome. *Cell* **121**, 887–898.

[29] Kumata Y, Tada S, Yamanada Y, Tsuyama T, Kobayashi T, Dong YP, Ikegami K, Murofushi H, Seki M, and Enomoto T (2007). Possible involvement of RecQL4 in the repair of double-strand DNA breaks in *Xenopus* egg extracts. *Biochim Biophys Acta* **1773**, 556–564.

[30] Wu J, Capp C, Feng L, and Hsieh TS (2008). *Drosophila* homologue of the Rothmund-Thomson syndrome gene: essential function in DNA replication during development. *Dev Biol* **323**, 130–142.

[31] Schajowicz F, Sissons HA, and Sobin LH (1995). The World Health Organization's histologic classification of bone tumors. A commentary on the second edition. *Cancer* **75**, 1208–1214.

[32] Wang LL, Worley K, Gannavarapu A, Chintagumpala MM, Levy ML, and Plon SE (2002). Intron-size constraint as a mutational mechanism in Rothmund-Thomson syndrome. *Am J Hum Genet* **71**, 165–167.

[33] Petkovic M, Dietschy T, Freire R, Jiao R, and Stagljar I (2005). The human Rothmund-Thomson syndrome gene product, *RECQL4*, localizes to distinct nuclear foci that coincide with proteins involved in the maintenance of genome stability. *J Cell Sci* **118**, 4261–4269.

[34] Kitao S, Ohsugi I, Ichikawa K, Goto M, Furuichi Y, and Shimamoto A (1998). Cloning of two new human helicase genes of the RecQ family: biological significance of multiple species in higher eukaryotes. *Genomics* **54**, 443–452.

[35] Yin J, Kwon YT, Varshavsky A, and Wang W (2004). *RECQL4*, mutated in the Rothmund-Thomson and RAPADILINO syndromes, interacts with ubiquitin ligases UBR1 and UBR2 of the N-end rule pathway. *Hum Mol Genet* **13**, 2421–2430.

[36] Finke J, Fritzen R, Ternes P, Lange W, and Dolken G (1993). An improved strategy and a useful housekeeping gene for RNA analysis from formalin-fixed, paraffin-embedded tissues by PCR. *Biotechniques* **14**, 448–453.

[37] Olshen AB, Venkatraman ES, Lucito R, and Wigler M (2004). Circular binary segmentation for the analysis of array-based DNA copy number data. *Biostatistics* **5**, 557–572.

[38] Sirvent N, Coindre JM, Maire G, Hostein I, Keslair F, Guillou L, Ranchere-Vince D, Terrier P, and Pedeutour F (2007). Detection of MDM2-CDK4 amplification by fluorescence *in situ* hybridization in 200 paraffin-embedded tumor samples: utility in diagnosing adipocytic lesions and comparison with immunohistochemistry and real-time PCR. *Am J Surg Pathol* **31**, 1476–1489.

[39] Ventura RA, Martin-Subero JI, Jones M, McParland J, Gesk S, Mason DY, and Siebert R (2006). FISH analysis for the detection of lymphoma-associated chromosomal abnormalities in routine paraffin-embedded tissue. *J Mol Diagn* **8**, 141–151.

[40] Rossi E, Ubiali A, Balzarini P, Cadei M, Alpi F, and Grigolatoi PG (2005). High-level detection of gene amplification and chromosome aneuploidy in extracted nuclei from paraffin-embedded tissue of human cancer using FISH: a new approach for retrospective studies. *Eur J Histochem* **49**, 53–58.

[41] Ying KL, Oizumi J, and Curry CJ (1990). Rothmund-Thomson syndrome associated with trisomy 8 mosaicism. *J Med Genet* **27**, 258–260.

[42] Der Kaloustian VM, McGill JJ, Vekemans M, and Kopelman HR (1990). Clonal lines of aneuploid cells in Rothmund-Thomson syndrome. *Am J Med Genet* **37**, 336–339.

[43] Orstavik KH, McFadden N, Hagelsteen J, Ormerod E, and van der Hagen CB (1994). Instability of lymphocyte chromosomes in a girl with Rothmund-Thomson syndrome. *J Med Genet* **31**, 570–572.

[44] Miozzo M, Castorina P, Riva P, Dalpra L, Fuhrman Conti AM, Volpi L, Hoe TS, Khoo A, Wiegant J, Rosenberg C, et al. (1998). Chromosomal instability in fibroblasts and mesenchymal tumors from 2 sibs with Rothmund-Thomson syndrome. *Int J Cancer* **77**, 504–510.

[45] Lindor NM, Devries EM, Michels VV, Schad CR, Jalal SM, Donovan KM, Smithson WA, Kvols LK, Thibodeau SN, and Dewald GW (1996). Rothmund-Thomson syndrome in siblings: evidence for acquired *in vivo* mosaicism. *Clin Genet* **49**, 124–129.

[46] Nishijo K, Nakayama T, Aoyama T, Okamoto T, Ishibe T, Yasura K, Shima Y, Shibata KR, Tsuboyama T, Nakamura T, et al. (2004). Mutation analysis of the *RECQL4* gene in sporadic osteosarcomas. *Int J Cancer* **111**, 367–372.

[47] Risinger MA and Groden J (2004). Crosslinks and crosstalk: human cancer syndromes and DNA repair defects. *Cancer Cell* **6**, 539–545.

[48] German J (1993). Bloom syndrome: a mendelian prototype of somatic mutational disease. *Medicine (Baltimore)* **72**, 393–406.

[49] Goto M, Miller RW, Ishikawa Y, and Sugano H (1996). Excess of rare cancers in Werner syndrome (adult progeria). *Cancer Epidemiol Biomarkers Prev* **5**, 239–246.

[50] Larizza L, Magnani I, and Roversi G (2006). Rothmund-Thomson syndrome and *RECQL4* defect: splitting and lumping. *Cancer Lett* **232**, 107–120.

[51] Kuhn EM and Therman E (1986). Cytogenetics of Bloom's syndrome. *Cancer Genet Cytogenet* **22**, 1–18.

[52] Hoehn H, Bryant EM, Au K, Norwood TH, Boman H, and Martin GM (1975). Variegated translocation mosaicism in human skin fibroblast cultures. *Cytogenet Cell Genet* **15**, 282–298.

[53] Liu Y, El-Naggar S, Clem B, Chesney J, and Dean DC (2008). The Rb/E2F pathway and Ras activation regulate RecQ helicase gene expression. *Biochem J* **412**, 299–306.

[54] Linton KM, Hey Y, Saunders E, Jeziorska M, Denton J, Wilson CL, Swindell R, Dibben S, Miller CJ, Pepper SD, et al. (2008). Acquisition of biologically relevant

gene expression data by Affymetrix microarray analysis of archival formalin-fixed paraffin-embedded tumours. *Br J Cancer* **98**, 1403–1414.

[55] Thomassen M, Tan Q, and Kruse TA (2008). Gene expression meta-analysis identifies chromosomal regions and candidate genes involved in breast cancer metastasis. *Breast Cancer Res Treat*; [Epub ahead of print].

[56] Saglam O, Shah V, and Worsham MJ (2007). Molecular differentiation of early and late stage laryngeal squamous cell carcinoma: an exploratory analysis. *Diagn Mol Pathol* **16**, 218–221.

[57] Buffart TE, Coffa J, Hermsen MA, Carvalho B, van der Sijp JR, Ylstra B, Pals G, Schouten JP, and Meijer GA (2005). DNA copy number changes at 8q11-24 in metastasized colorectal cancer. *Cell Oncol* **27**, 57–65.

[58] Narayan G, Bourdon V, Chaganti S, Arias-Pulido H, Nandula SV, Rao PH, Gissmann L, Durst M, Schneider A, Pothuri B, et al. (2007). Gene dosage alterations revealed by cDNA microarray analysis in cervical cancer: identification of candidate amplified and overexpressed genes. *Genes Chromosomes Cancer* **46**, 373–384.

[59] Coindre JM, Hostein I, Maire G, Derre J, Guillou L, Leroux A, Ghnassia JP, Collin F, Pedeutour F, and Aurias A (2004). Inflammatory malignant fibrous histiocytomas and dedifferentiated liposarcomas: histological review, genomic profile, and MDM2 and CDK4 status favour a single entity. *J Pathol* **203**, 822–830.

[60] Mai S and Mushinski JF (2003). c-Myc–induced genomic instability. *J Environ Pathol Toxicol Oncol* **22**, 179–199.

Table W1. Identification of N-CIN and S-CIN in Study Group of 10 OS.

Chromosome	Cytoband		Aberration Location ↔ CIN Type	
			N-CIN	S-CIN
chr1	p36.33	Telomere		
	p12 -p36.32	Arm		
	p11.2	Centromere		
	q21.1	Centromere		
	q21.2-q43	Arm		
	q44	Telomere		
chr2	p25.3	Telomere		
	p12-p25.2	Arm		
	p11.2	Centromere		
	q11.2	Centromere		
	q12.1-q37.2	Arm		
	q37.3	Telomere		
chr3	p26.3	Telomere		
	p11.2-p26.2	Arm		
	p11.1	Centromere		
	q11.2	Centromere		
	q12.1-q28	Arm		
	q29	Telomere		
chr4	p16.3	Telomere		
	p13-q16.2	Arm		
	p12	Centromere		
	q11	Centromere		
	q12-q35.1	Arm		
	q35.2	Telomere		
chr5	p15.33	Telomere		
	p12-p15.32	Arm		
	p11	Centromere		
	q11.1	Centromere		
	q11.2-q35.3	Arm		
	q35.3	Telomere		
chr6	p25.3	Telomere		
	p12.1-p25.2	Arm		
	p11.2	Centromere		
	q11.1	Centromere		
	q11.2-q26	Arm		
	q27	Telomere		
chr7	p22.3	Telomere		
	p11.2-p22.2	Arm		
	p11.1	Centromere		
	q11.21	Centromere		
	q11.22-q35.2	Arm		
	q36.3	Telomere		
chr8	p23.3	Telomere		
	p11.22-p23.2	Arm		
	p11.21	Centromere		
	q11.1	Centromere		
	q11.21-q24.2	Arm		
	q24.3	Telomere		
chr9	p24.3	Telomere		
	p13.2-p24.2	Arm		
	p13.1	Centromere		
	p12	Centromere		
	q12	Centromere		
	q13	Centromere		
	q21.11-q34.2	Arm		
	q34.3	Telomere		
chr10	p15.3	Telomere		
	p11.22-q15.2	Arm		
	p11.21	Centromere		
	q11.21	Centromere		
	q11.22-q26.2	Arm		
	q26.3	Telomere		
chr11	p15.5	Telomere		
	p11.2-p15.4	Arm		
	p11.12	Centromere		
	q11	Centromere		
	q12.1-q24.3	Arm		
	q25	Telomere		

Table W1. (*continued*)

Chromosome	Cytoband		Aberration Location ↔ CIN Type	
			N-CIN	S-CIN
chr12	p13.33	Telomere		
	p11.21-p13.32	Arm		
	p11.1	Centromere		
	q12	Centromere		
	q13.11-q24.32	Arm		
	q24.33	Telomere		
chr13	q12.11	Centromere		
	q12.12-q33.33	Arm		
	q34	Telomere		
chr14	q11.1	Centromere		
	q11.2-q32.32	Arm		
	q32.33	Telomere		
chr15	q11.2	Centromere		
	q12-q26.2	Arm		
	q26.3	Telomere		
chr16	p13.3	Telomere		
	p12.1-p13.2	Arm		
	p11.2	Centromere		
	q12.1	Centromere		
	q12.2-q24.2	Arm		
	q24.3	Telomere		
chr17	p13.3	Telomere		
	p12-13,2	Arm		
	p11.2	Centromere		
	q11.1	Centromere		
	q11.2-q25.2	Arm		
	q25.3	Telomere		
chr18	p11.32	Telomere		
	p11.22-p11.31	Arm		
	p11.21	Centromere		
	q11.2	Centromere		
	q12.1-q22.3	Arm		
	q23	Telomere		
chr19	P13.3	Telomere		
	p13.11-p13.2	Arm		
	p12	Centromere		
	q12	Centromere		
	q13.11-q13.42	Arm		
	q13.43	Telomere		
chr20	p13	Telomere		
	p11.22-p12.3	Arm		
	p11.21	Centromere		
	q11.21	Centromere		
	q11.22-q13.32	Arm		
	q13.33	Telomere		
chr21	p11.1	Centromere		
	q11.2	Centromere		
	q21.1-q22.2	Arm		
	q22.3	Telomere		
chr22	q11.1	Centromere		
	q11.21-q13.32	Arm		
	q13.33	Telomere		

The position of genomic imbalance from all 10 OS is shown by cytoband location. Structural aberrations leading to S-CIN imbalance is mapped by black boxes and N-CIN imbalance is indicated by gray boxes.

Table W2. Estimation of the Overall Ploidy of 10 Samples.

OS	cen(3),* *n* (%)	cen(7),* *n* (%)	cen(17),* *n* (%)	Overall Ploidy Status†
OS1	2 (60%)	2 (70%)	2 (70%)	Diploid
	3 (15%)	3 (>10%)	3 (15%)	
	4 (<10%)			
OS4	1 (30%)	2 (60%)	2 (60%)	Diploid
	2 (60%)	3 (20%)	3 (20%)	
OS5	2 (70%)	2 (50%)	2 (40%)	Near-triploid
	3 (>10%)	3 (20%)	3 (40%)	
			4 (>10%)	
OS7	2	2 (50%)	2 (35%)	Near-triploid
		3 (20%)	3 (40%)	
		4 (>10%)	4 (>10%)	
OS9	2	2 (60%)	2 (>10%)	Polyploid (>5 n)
		3 (>10%)	3 (20%)	
		>5 (60%)		
OS11	2	2 (60%)	2 (70%)	Diploid
		3 (15%)	3 (>10%)	
OS12	2 (80%)	2 (30%)	3 (>10%)	Near-tetraploid
	3 (>10%)	3 (30%)	4 (20%)	
		4 (20%)	5 (20%)	
		5 (>10%)	>5 (30%)	
OS13	2	2 (50%)	ND	Diploid
		4 (15%)		
OS15	1 (30%)	2 (50%)	2 (40%)	Near-tetraploid
	2 (60%)	3 (20%)	3 (30%)	
		4 (20%)	4 (20%)	
OS18	2 (70%)	2 (53%)	2 (60%)	Near-triploid
	3 (>10%)	3 (27%)	3 (20%)	
		4 (>10%)		

*For each sample, 200 nuclei were scored, and a population of cell was recorded if it was represented by more than 10% of the cells.

†Overall ploidy criteria are established according to Ventura et al. [39], with modification described in the Materials and Methods section.